Correlation of Magnetic Resonance Imaging With Knee Anterolateral Ligament Anatomy

A Cadaveric Study

Camilo Partezani Helito,*[†] MD, Paulo Victor Partezani Helito,[‡] MD, Marcelo Batista Bonadio,[†] MD,
José Ricardo Pécora,[†] MD, PhD, Marcelo Bordalo-Rodrigues,[‡] MD,
Gilberto Luis Camanho,[†] MD, PhD, and Marco Kawamura Demange,[†] MD, PhD
Investigation performed at the Department of Orthopedics and Traumatology, Faculty of Medicine, University of São Paulo, São Paulo, Brazil

Background: Anatomic and magnetic resonance imaging (MRI) studies have recently characterized the knee anterolateral ligament (ALL). So far, no study has focused on confirming whether the evaluated MRI parameters truly correspond with ALL anatomy.

Purpose: To assess the validity of MRI in detecting the ALL using an anatomic evaluation as reference.

Study Design: Descriptive laboratory study.

Methods: A total of 13 cadaveric knees were subjected to MRI and then to anatomic dissection. Dissection was performed according to previous anatomic study methodology. MRIs were performed with a 0.6- to 1.5-mm slice thickness and prior saline injection. The following variables were analyzed: distance from the origin of the ALL to the origin of the lateral collateral ligament (LCL), distance from the origin of the ALL to its bifurcation point, maximum length of the ALL, distance from the tibial insertion of the ALL to the articular surface of the tibia, ALL thickness, and ALL width. The 2 sets of measurements were analyzed using the Spearman correlation coefficient (ρ) and Bland-Altman plots.

Results: The ALL was clearly observed in all dissected knees and MRI scans. It originated anterior and distal to the LCL, close to the lateral epycondile center, and showed an anteroinferior path toward the tibia, inserting between the Gerdy tubercle and the fibular head, around 5 mm under the lateral plateau. The ρ values tended to increase together for all studied variables between the 2 methods, and all were statistically significant, except for thickness ($P = .077$). Bland-Altman plots showed a tendency toward a reduction of ALL thickness and width by MRI compared with anatomic dissection.

Conclusion: MRI scanning as described can accurately assess the ALL and demonstrates characteristics similar to those seen under anatomic dissection.

Clinical Relevance: MRI can accurately characterize the ALL in the anterolateral region of the knee, despite the presence of structures that might overlap and thus cause confusion when making assessments based on imaging methods.

Keywords: anterolateral ligament; magnetic resonance imaging; MRI; anatomy

Recent anatomic studies have clearly established the landmarks for locating the origin and insertion of the knee anterolateral ligament (ALL), as well as its path and characteristics.[1,4,6,10,15,24,28] According to the literature, the origin of the ALL is close to the center of the lateral epicondyle, between the origin of the lateral collateral ligament (LCL) and the insertion of the popliteus muscle tendon (PMT) or slightly proximal and posterior to the lateral epicondyle. The ALL then goes in an anteroinferior direction toward the tibia, having an insertion between the fibular head and Gerdy tubercle.[8,11,17] Some authors also found an attachment to the lateral meniscus.[9] The ALL has recently been praised for its possible role as a stabilizer of knee rotation, according to biomechanical studies performed by Monaco et al[20-22] and clinical studies that have added lateral procedures to conventional intra-articular anterior cruciate ligament (ACL) reconstructions.[5,26,27]

Despite the anatomic and biomechanical studies available, few studies have assessed the ALL using imaging methods, particularly magnetic resonance imaging (MRI), which is the standard method for assessment of knee ligaments.[1,2,12,14] Three recent studies investigated the ALL using MRI, 2 of which examined individuals without a ligament injury and the third examined individuals with an

TABLE 1
Parameters Used in the MRI Sequences[a]

MRI Sequence	MRI Parameter										
	TE, ms	TR, ms	ETL, n	BW, Hz	Frequency, Hz	Phase, n	NEX, n	FOV, cm	Spacing, cm	Thickness, mm
Sagittal PDW	38	2267	9	19.23	288	192	2	12	0.0	1.5
Coronal PDW	38	4300	10	31.25	288	192	4	12	0.0	1.2
Axial PDW	38	2384	9	19.23	288	192	2	11	0.0	1.5
Coronal 3D T2W	—	1500	64	125	224	224	1	18	—	0.6

[a]3D, 3-dimensional; BW, bandwidth; ETL, echo train length; FOV, field of view; MRI, magnetic resonance imaging; NEX, number of excitations; PDW, proton density–weighted; T2W, T2-weighted; TE, echo time; TR, repetition time.

ACL injury. All 3 studies found that the ALL could not be observed in its entirety in approximately 25% of cases.[2,12,14]

To the best of our knowledge, no study has studied the anatomic-radiological correlation for the characterization of the ALL with objective measurements using the same knees; that is, comparing the measurements obtained from anatomic specimens and magnetic resonance scans performed on the same knees prior to dissection. Such characterization is relevant because the knee includes several structures that might overlap and thus cause confusion when making assessments based on imaging methods.

Therefore, the purpose of this study was to assess the validity of an experimental MRI protocol with a small slice thickness and saline injection into the joint in detecting the ALL using anatomic evaluation as reference. We hypothesized that MRI is a valid instrument to detect the anatomy of the ALL.

METHODS

This laboratory study was conducted using 13 consecutive cadaveric knees. The study was approved by the institutional research ethics committee of our institution. All of the cadavers were males with a mean (±SD) of 66.0 ± 10.0 years (range, 49-82 years). All cadavers were subjected to MRI and then to anatomic dissection. Anatomic dissections were performed immediately after MRI, before interpretation of imaging results.

All MRI scans were performed using a 1.5-T MR imager (Signa Excite HD; GE Healthcare) with a dedicated knee coil (HD TRKnee 8 Ch High-Resolution Knee Array). Slice thickness was set at 0.6 to 1.5 mm, with no spacing between images. The knees were held in 15° of flexion according to the MRI equipment protocol, with neutral rotation. All knees were subjected to an intra-articular injection of 40 mL of saline solution before image acquisition to distend the joint capsule and thus facilitate the observation of the ALL. All injections were performed with a lateral suprapatellar

approach by one of the authors (P.V.P.H.) with the knee in full extension. The scans were performed 10 minutes after injection and included an MRI knee imaging protocol with axial, sagittal, and coronal proton density–weighted sequences and a volumetric T2-weighted coronal sequence. The MRI parameters are described in Table 1.

The MRI scans were assessed using a picture archiving and communication system workstation, and the following measurements were performed: linear distance from the origin of the ALL to the origin of the LCL; distance from the origin of the ALL to its bifurcation point, when fibers connect to the lateral meniscus; maximum length of the ALL (measured as the distance between its origin and tibial insertion); distance from the tibial insertion of the ALL to the articular surface of the tibia; thickness; and width of the ALL (Figures 1-3). Measurements of width and thickness were performed close to the joint line, above the level of the lateral meniscus. All measurements were performed in coronal sequences, except for thickness and width, which were measured in axial sequences. Two authors with experience in musculoskeletal radiology (P.V.P.H., M.B.R.) analyzed the MRI scans separately. They performed 2 measurements at least 15 days apart. Inter- and intraobserver correlation coefficients were calculated.

Following MRI, the cadavers were dissected according to a protocol established in previous studies.[10,15] The procedure began with the dissection of the skin and subcutaneous tissue, followed by tenotomy of the quadriceps tendon, opening of the joint by means of a medial parapatellar approach, and tibial tubercle osteotomy to gain access to the knee anterolateral area without disrupting the adjacent soft tissue. Next, resection of the iliotibial tract at the Gerdy tubercle was performed followed by isolating the ALL proximally to distally based on its origin location anterior to the LCL. The origin of the ALL was carefully separated from the origin of the LCL. The ALL was not separated from the lateral meniscus, and its fibers between the body and anterior horn of the lateral meniscus, a possible true attachment, were preserved. When the ALL was isolated, all adjacent structures were removed except the

*Address correspondence to Camilo Partezani Helito, MD, Rua Dr Ovídio Pires de Campos, 333, Cerqueira Cesar, São Paulo, SP-CEP: 05403-010, Brazil (email: camilo_helito@yahoo.com.br).

†Department of Orthopaedics and Traumatology, Knee Surgery Division, Institute of Orthopedics and Traumatology–Hospital and Clinics, Faculty of Medicine, University of São Paulo (IOT-HCFMUSP), São Paulo, Brazil.

‡Department of Orthopaedics and Traumatology, Musculoskeletal Radiology Division, Institute of Orthopedics and Traumatology–Hospital and Clinics, Faculty of Medicine, University of São Paulo (IOT-HCFMUSP), São Paulo, Brazil.
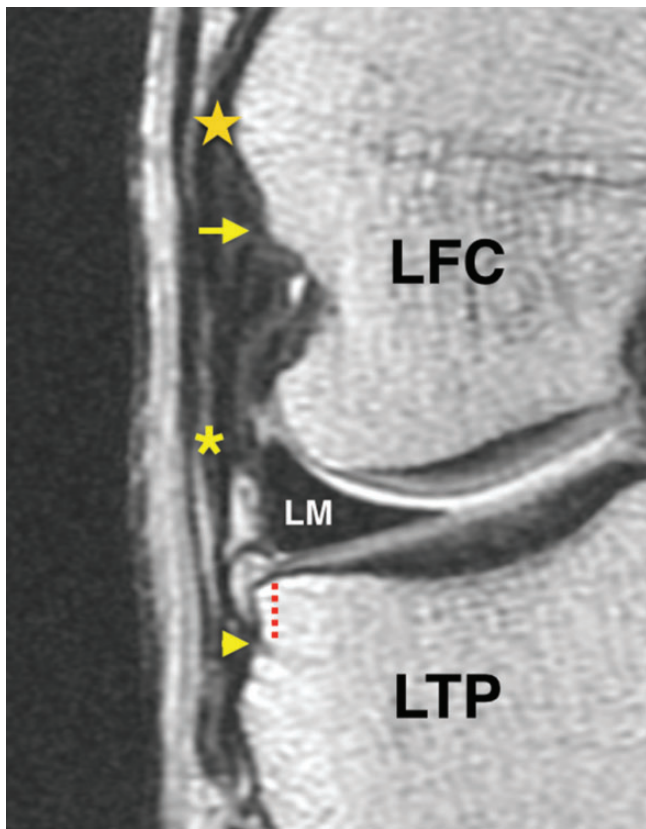
Figure 1. Coronal proton density–weighted section of the right knee showing the origin of the lateral collateral ligament (star); the origin (arrow), bifurcation point (asterisk), and tibial insertion (arrowhead) of the anterolateral ligament; and the distance from the tibial insertion to the lateral plateau (dotted line). LFC, lateral femoral condyle; LM, lateral meniscus; LTP, lateral tibial plateau.

LCL, including the remaining portions of the lateral capsule, for better visualization. All dissections were performed by 2 authors together (C.P.H., M.B.B.).

Once the ALL was isolated, the following measurements were performed with a digital caliper: distance from the origin of the ALL to the origin of the LCL in the lateral femoral condyle, distance from the origin of the ALL to its bifurcation point, distance from the tibial insertion of the ALL to the lateral tibial plateau cartilage, total length of the ALL (measured as the distance between its origin and tibial insertion), and thickness and width of the ALL—the same measurements that had been performed on the MRI scans. Measurements were performed with approximately 15° of knee flexion and neutral rotation, similar to the knee position in the MRI studies. The width and thickness measurements were performed above the level of the lateral meniscus, similar to the measurements performed using MRI. Anatomic measurements were performed by 2 authors independently (C.P.H., M.B.B.). Interobserver correlation of measurements was calculated.

The 2 sets of measurements (MRI and anatomic specimens) were subjected to statistical analysis using SPSS
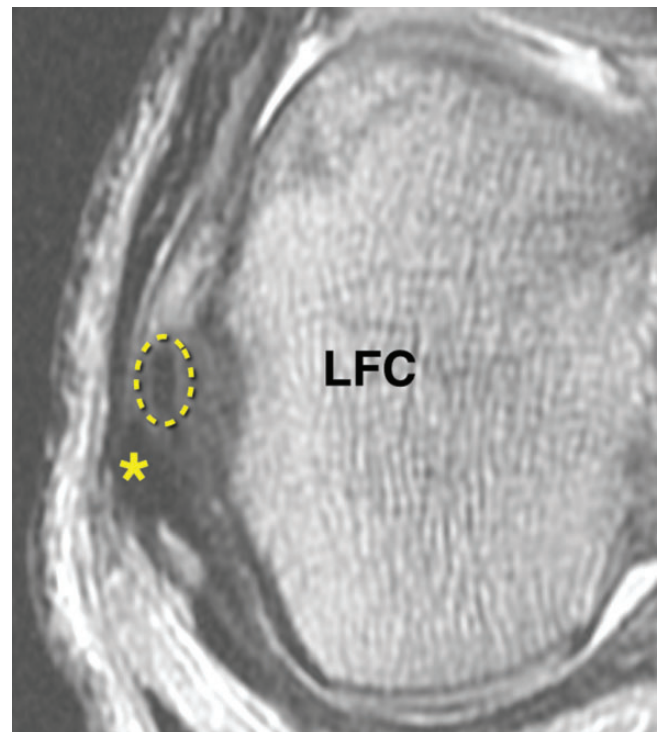

Figure 2. Axial proton density–weighted section of the right knee showing the anterolateral ligament (dotted oval) located anterior to the lateral collateral ligament (asterisk) at the level of the lateral femoral condyle (LFC).
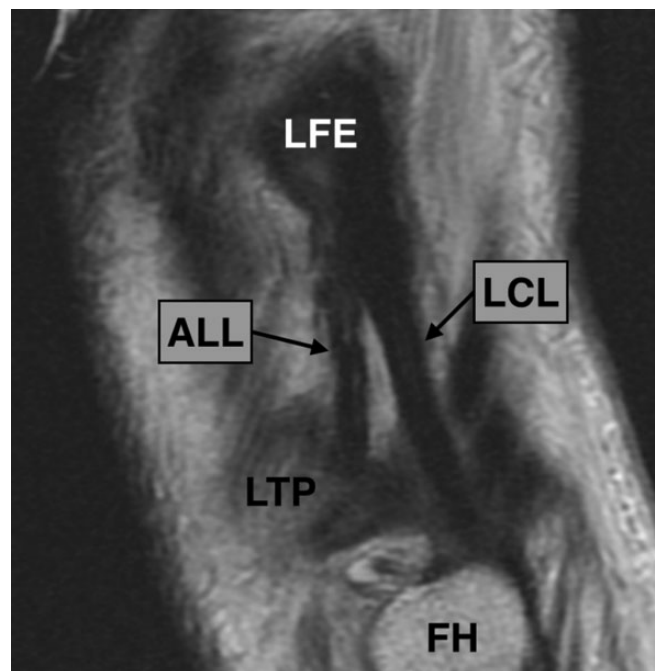

Figure 3. Sagittal proton density–weighted section of the right knee showing the relationship between the anterolateral ligament (ALL) and the lateral collateral ligament (LCL). The origins of both are close to the lateral femoral epicondyle (LFE), but the ALL runs anteriorly to the LCL and inserts in the lateral tibial plateau (LTP) while the insertion of the LCL is in the fibular head (FH).
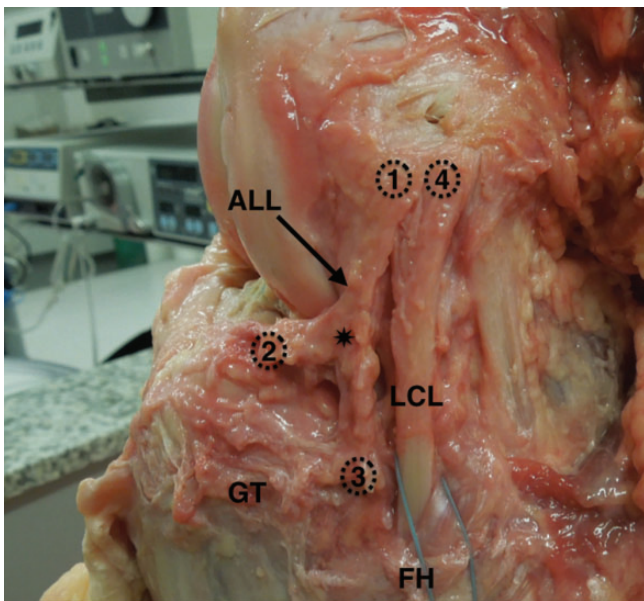
Figure 4. Anatomic photograph of a cadaveric left knee from a lateral view showing the origin of the anterolateral ligament (ALL) (1) located close to the origin of the lateral collateral ligament (LCL) (4). The ALL travels in an anteroinferior direction toward the tibia and bifurcates (asterisk) before its insertions in the meniscus (2) and the tibia (3). GT, Gerdy tubercle; FH, fibular head.
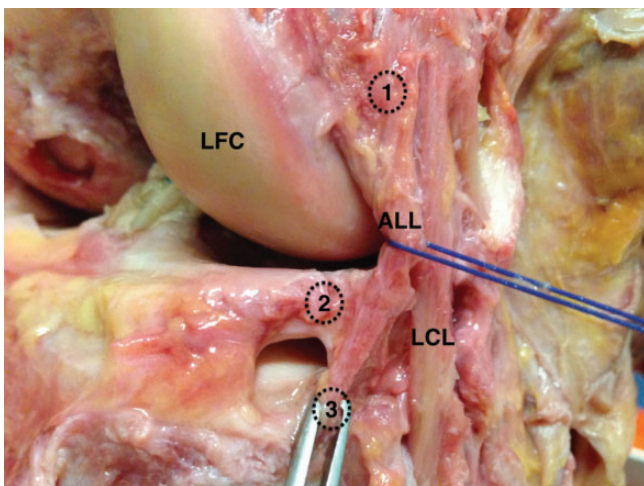

Figure 5. Anatomic photograph of a cadaveric left knee from an anterolateral view showing the origin (1) and tibial insertion (3) of the knee anterolateral ligament (ALL). The ALL is surrounded by the blue suture. The lateral meniscus is indicated by (2). LCL, lateral collateral ligament; LFC, lateral femoral condyle.

20.0 software (IBM Corp). The Spearman correlation coefficient (ρ) was calculated with the corresponding 95% confidence interval ($P < .05$). In addition, a comparative analysis of the correlation between the 2 sets of measurements was performed using Bland-Altman plots.

TABLE 2
Measurements of Anatomic Specimens and
MRI Scans With Spearman Correlation Coefficient
for the Investigated Variables[a]

	Method, Mean ± SD			
	Anatomy	MRI	ρ	P
Distance from origin to the LCL, mm	3.77 ± 1.481	3.92 ± 1.935	0.932	<.001
Distance from origin to the bifurcation point, mm	18.46 ± 3.406	17.92 ± 2.691	0.939	<.001
Distance from the insertion to the tibial plateau, mm	5.38 ± 1.446	5.46 ± 1.266	0.877	<.001
Length, mm	36.62 ± 4.053	36.15 ± 3.76	0.943	<.001
Thickness, mm	2.23 ± 0.439	1.54 ± 0.519	0.507	.077
Width, mm	6.08 ± 1.038	5.23 ± 0.725	0.875	<.001

[a]ρ, Spearman correlation coefficient; LCL, lateral collateral ligament; MRI, magnetic resonance imaging.

RESULTS

The ALL was clearly observed on macroscopic inspection (gross anatomy) in all 13 dissected knees. The entire path of the ALL was also visualized in all of the MRI scans (Figures 4 and 5). The anatomic and MRI measurements are provided in Table 2.

The attachment of the ALL in the lateral epicondyle region was found anterior and distal to the attachment of the LCL. The ligament then coursed anterodistally to the proximal anterolateral tibial region, attaching between the Gerdy tubercle and the fibular head 5.3 mm under the lateral tibial plateau. Close proximity to the lateral meniscus was observed during its course.

Through use of MRI, the ALL was characterized with greater clarity on the coronal and axial planes as a thin linear structure with a thickness varying between 1 and 2 mm and surrounded by adipose tissue or synovial fluid. The origin of the ALL on the outer face of the lateral femoral condyle was located immediately anterior to the LCL.

The ALL showed an anteroinferior path, superficial to the origin of the popliteal tendon groove. A bifurcation could be observed above the lateral inferior geniculate artery, leading to a meniscus and a tibial insertion. The tibial segment of the ALL was inserted 5.4 mm beneath the plane of the lateral tibial plateau and under the insertion of the iliotibial tract.

Interobserver correlation for anatomic measurements varied between 0.86 and 0.96. Intra- and interobserver correlation for MRI measurements were 0.77 to 0.93 and 0.85 to 0.90, respectively.

With regard to the correlation between the anatomic and MRI findings, the correlation coefficient (ρ) was between 0 and 1 for all studied variables, denoting that the 2 values tended to increase or decrease together. All values were statistically significant except for ALL thickness ($P = .077$), which showed a minor correlation coefficient (ρ = 0.507) between methods.
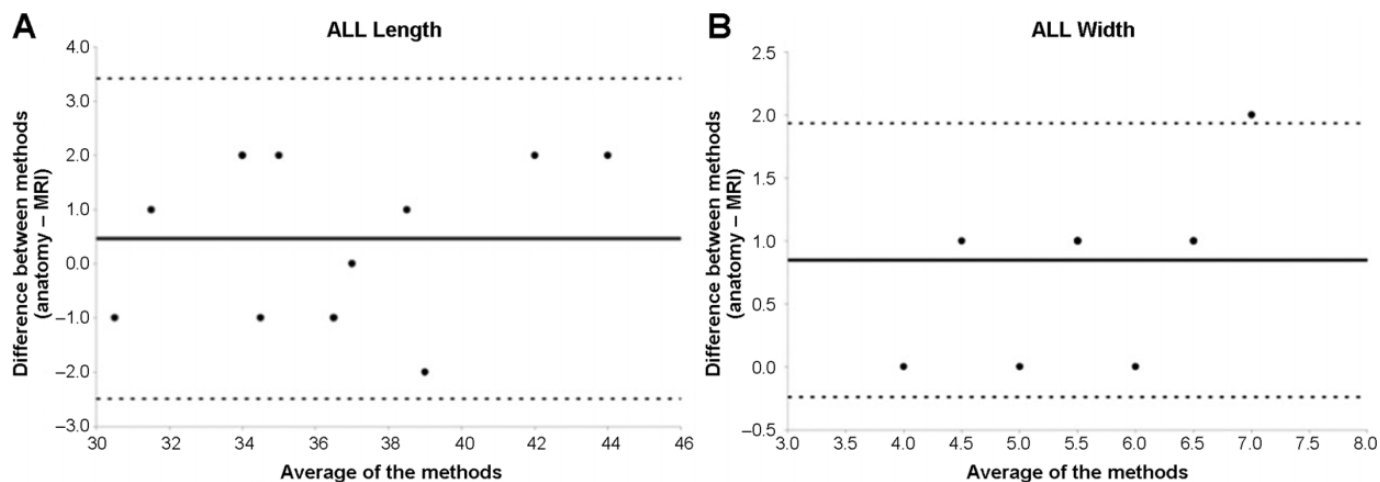
Figure 6. Bland-Altman plot analysis for (A) length and (B) width of the knee anterolateral ligament (ALL). The width analysis, measured close to the joint line level, shows that magnetic resonance imaging (MRI) tends to measure reduced ALL values compared with anatomic measurements.

TABLE 3
MRI Protocols Used in This Study Compared With Previous Anterolateral Ligament Studies Using MRI[a]

Study	Study Type	Strength, T	Sequences	Spacing, mm	Thickness, mm
			MRI Protocol		
Caterine et al[1]	Cadavers	3.0	Coronal 3D T1	—	0.4
Claes et al[2]	Living subjects	—	Coronal T2	—	—
Helito et al[14]	Living subjects	1.5	Coronal T1, sagittal T1, axial T2, sagittal T2, coronal T2, coronal PDW	0.3-0.5	2-3.5
Current study	Cadavers	1.5	Axial PDW, sagittal PDW, coronal PDW, coronal 3D T2	0.0	0.6-1.5

[a]3D, 3-dimensional; MRI, magnetic resonance imaging; PDW, proton density–weighted.

Looking for variation trends between the 2 sets of measurements, an analysis by means of Bland-Altman plots showed that MRI tends to measure reduced ALL thickness and width values compared with anatomic measurements. For the other variables, different values between methods, on average, were close to 0, and it was not possible to observe any trend in values between the 2 methods studied (MRI and anatomy) (Figure 6).

DISCUSSION

This study demonstrated excellent correlation between the findings by anatomic dissection of the ALL and MRI scans. The main clinical relevance of this study in validating MRI for ALL assessment is that due to several structures that might overlap in the lateral portion of the knee, confusion can be caused when making assessments based on imaging methods. This study could objectively quantify and compare findings by MRI and anatomy.

The study by Caterine et al[1] using MRI of cadavers also succeeded in observing the ALL in all the investigated knees, in contrast to the studies conducted with living subjects in which the ALL could not be characterized in its entirety.[2,12,14] We believe that this discrepancy between studies with cadavers and living subjects is due to the imaging protocols used, with sequences with smaller slice thicknesses used in the MRI scans of anatomic specimens. The slice thickness of 0.6 to 1.5 mm, with no spacing between images, enabled us to visualize the ALL even with a 1.5-T MRI protocol (Table 3).

Correlation between methods was weak for ALL thickness, and an analysis of the Bland-Altman plots showed a tendency toward smaller values measured by MRI compared with those found during anatomic dissection. A possible explanation for this tendency for errors is the difficulty of achieving full dissection of the soft tissue around the ligament, with a consequent increase of the thickness and width values in cadaveric specimens. This fact must be taken into account when doing ALL assessment by MRI. Another hypothesis for this weak correlation is that it is not always easy to define the boundaries of the ALL during dissection due to its close relation to the anterolateral capsule.

Although there has not been a clinical study showing the importance of the ALL in rotatory knee stability, biomechanical studies performed by Monaco et al[20,22] found

increased grade on the pivot-shift test when injury to the anterolateral portion of the joint capsule was performed. Those authors analyzed the ALL indirectly, in our opinion. Monaco et al[21] also showed that extra-articular tenodesis associated with single-bundle ACL reconstruction is more effective in reducing tibial internal rotation when compared with double-bundle ACL reconstruction. These studies highlight the importance that has been recently attributed to the ALL for its possible role as a stabilizer of knee rotation. Müller[23] has also described the anterolateral femorotibial ligament, a lateral ligamentous complex similar to the recently described ALL. This author recommended techniques to repair and reconstruct this lateral complex injury with the aim to enhance knee stability.

Characterization of the ALL by preoperative MRI scans is relevant for the assessment of the possible reconstruction of this ligament. Although certain parameters for reconstruction have been formulated,[11,13,25] there is not yet a definite criterion for combined reconstruction of the ALL and ACL. Even in the case of extra-articular reconstructions, for which several techniques were described, there is not yet a consensus in the literature as to the precise indication for that procedure.[5,16,21,26,27] Duthon et al[7] considered extra-articular reconstruction relevant, particularly in cases of revision of ACL reconstruction, patients with gross pivot shift, and individuals who practice sports that require knee rotation. McGuire and Wolchok[19] considered an extra-articular reconstruction for revision ACL reconstructions and add as possible indications previous lateral extra-articular reconstructions with persistent knee instability and knee dislocations. The characterization of ALL injuries might provide an indication for reconstruction, and the identification of anatomic and MRI landmarks can improve development of future reconstruction techniques. As no published study has yet investigated the healing ability of the ALL, it is not possible to predict whether all lesions identified on imaging tests will systematically develop anterolateral instability over time, thus requiring reconstruction.

Our anatomic dissection results differed from the study performed by Dodds et al[6] in relation to the femoral ALL attachment, which found the origin point of the ALL was located 4.3 mm posterior and 8.0 mm proximal to the LCL femoral attachment. We found the ALL anterior and distal to the LCL femoral attachment close to the center of the lateral epicondyle, similar to Helito et al[10] (2.2 mm anterior and 3.5 mm distal) and Claes et al.[4] Caterine et al[1] found 2 patterns of the ALL femoral attachment, but the most common was similar to that shown in this study. Dodds et al[6] did not perform histological analysis of the femoral attachment, as was done by Caterine et al[1] and Helito et al.[10] The tibial attachment site was similar to all previous studies.[1,4,6,10] According to our dissections, a close proximity to the lateral meniscus was observed, similar to the study performed by Helito et al[9] that characterized this attachment in detail, including histological analysis.

Caterine et al[1] subjected cadavers to MRI in an attempt to characterize the ALL; however, they performed a macroscopic comparison of the MRI and the anatomic findings only. Our study included objective comparison measurements done not only in the anatomic specimens but also in MRI. We believe that this study demonstrates that even though there are some structures located close to the ALL in the anterolateral region of the knee, it is possible to clearly delineate the ALL with MRI scans under the conditions in which the MRI was performed. Claes et al[3] compared anatomic measurements performed in cadavers and MRI scans of the knees of patients to establish whether a Segond fracture corresponded with the topography of ALL avulsion. Their results demonstrated that the ALL is attached to the tibial avulsion fracture fragment associated with ACL injury. The methods used by Claes et al[3] to compare the anatomic measurements with those performed on imaging tests were similar to ours.

Our study is not without its limitations, however. So far, there is not a conclusion about the clinical significance of the ALL nor its specific treatment indications.[18] Additional limitations of this study include the small number of cadaveric specimens used and the use of a 1.5-T MRI device. Although this type of equipment allows fine sections and volumetric sequences, a 3.0-T device might afford greater detail of the ALL and adjacent structures. The injection of saline solution can also be considered a limitation to the experimental setup performed as well as the slice thickness used, as this is not routine for MRI acquisition and may not be practical for clinical use. Another limitation is that only male specimens were used, so there are no data on female knees.

CONCLUSION

MRI scanning can accurately assess the anterolateral knee ligament and demonstrates findings similar to those obtained from anatomic dissection.

REFERENCES

1. Caterine S, Litchfield R, Johnson M, Chronik B, Getgood A. A cadaveric study of the anterolateral ligament: re-introducing the lateral capsular ligament. *Knee Surg Sports Traumatol Arthrosc*. 2015;23: 3186-3195.
2. Claes S, Bartholomeeusen S, Bellemans J. High prevalence of anterolateral ligament abnormalities in magnetic resonance images of anterior cruciate ligament-injured knees. *Acta Orthop Belg*. 2014;80: 45-49.
3. Claes S, Luyckx T, Vereecke E, Bellemans J. The Segond fracture: a bony injury of the anterolateral ligament of the knee. *Arthroscopy*. 2014;30:1475-1482.
4. Claes S, Vereecke E, Maes M, Victor J, Verdonk P, Bellemans J. Anatomy of the anterolateral ligament of the knee. *J Anat*. 2013;223:321-328.
5. Dejour D, Vanconcelos W, Bonin N, Saggin PR. Comparative study between mono-bundle bone-patellar tendon-bone, double-bundle hamstring and mono-bundle bone-patellar tendon-bone combined with a modified Lemaire extra-articular procedure in anterior cruciate ligament reconstruction. *Int Orthop*. 2013;37:193-199.
6. Dodds AL, Halewood C, Gupte CM, Williams A, Amis AA. The anterolateral ligament: anatomy, length changes and association with the Segond fracture. *Bone Joint J*. 2014;96:325-331.
7. Duthon VB, Magnussen RA, Servien E, Neyret P. ACL reconstruction and extra-articular tenodesis. *Clin Sports Med*. 2013;32:141-153.

8. Guenther D, Griffith C, Lesniak B, et al. Anterolateral rotatory instability of the knee. *Knee Surg Sports Traumatol Arthrosc*. 2015;23:2909-2917.

9. Helito CP, Bonadio MD, Soares TQ, et al. The meniscal insertion of the knee anterolateral ligament [published online August 6, 2015]. *Surg Radiol Anat*. doi:10.1007/s00276-015-1533-5.

10. Helito CP, Demange MK, Bonadio MB, et al. Anatomy and histology of the knee anterolateral ligament. *Orthop J Sports Med*. 2013;1: 2325967113513546.

11. Helito CP, Demange MK, Bonadio MD, et al. Radiographic landmarks for locating the femoral origin and the tibial insertion of the knee anterolateral ligament. *Am J Sports Med*. 2014;42:2356-2362.

12. Helito CP, Demange MK, Helito PV, et al. Assessment of the knee anterolateral ligament of the knee by means of magnetic resonance imaging. *Rev Bras Ortop*. 2015;50:214-219.

13. Helito CP, Helito PV, Bonadio MB, et al. Evaluation of the anterolateral ligament length and isometric pattern with serial computer tomography. *Orthop J Sports Med*. 2014;2:2325967114562205.

14. Helito CP, Helito PV, Costa HP, et al. MRI evaluation of the anterolateral ligament of the knee: assessment in routine 1.5-T scans. *Skeletal Radiol*. 2014;43:1421-1427.

15. Helito CP, Miyahara HS, Bonadio MB, et al. Estudo anatômico do ligamento anterolateral do joelho. *Rev Bras Ortop*. 2013;48:368-373.

16. Imbert P. Minimally invasive extra-articular anterolateral reinforcement: a new technique. *Arthroscopy*. 2007;23:907.e1-907.e4.

17. Kennedy MI, Claes S, Fuso FA, et al. The anterolateral ligament: an anatomic, radiographic, and biomechanical analysis. *Am J Sports Med*. 2015;43:1606-1615.

18. Lubowitz JH, Provencher MT, Brand JC, Rossi MJ. The knee anterolateral ligament. *Arthroscopy*. 2014;11:1385-1388.

19. McGuire DA, Wolchok J. Extra-articular lateral reconstruction technique. *Arthroscopy*. 2000;16:553-557.

20. Monaco E, Ferretti A, Labianca L, et al. Navigated knee kinematics after cutting of the ACL and its secondary restraint. *Knee Surg Sports Traumatol Arthrosc*. 2012;20:870-877.

21. Monaco E, Labianca L, Conteduca F, De Carli A, Ferretti A. Double bundle or single bundle plus extraarticular tenodesis in ACL reconstruction? *Knee Surg Sports Traumatol Arthrosc*. 2007;15:1168-1174.

22. Monaco E, Maestri B, Conteduca F, Mazza D, Iorio C, Ferretti A. Extra-articular ACL reconstruction and pivot shift: in vivo dynamic evaluation with navigation. *Am J Sports Med*. 2014;42:1669-1674.

23. Müller W. *The Knee: Form, Function and Ligament Reconstruction*. Berlin, Germany: Springer; 1982.

24. Pomajzl R, Maerz T, Shams C, Guettler J, Bicos J. A review of the anterolateral ligament of the knee: current knowledge regarding its incidence, anatomy, biomechanics, and surgical dissection. *Arthroscopy*. 2015;31:583-591.

25. Rezansoff AJ, Caterine S, Spencer L, Tran MN, Litchfield RB, Getgood AM. Radiographic landmarks for surgical reconstruction of the anterolateral ligament of the knee. *Knee Surg Sports Traumatol Arthrosc*. 2015;23:3196-3201.

26. Trojani C, Beaufils P, Burdin G, et al. Revision ACL reconstruction: influence of a lateral tenodesis. *Knee Surg Sports Traumatol Arthrosc*. 2012;20:1565-1570.

27. Vadalà AP, Iorio R, De Carli A, et al. An extra-articular procedure improves the clinical outcome in anterior cruciate ligament reconstruction with hamstrings in female athletes. *Int Orthop*. 2013;37: 187-192.

28. Vincent JP, Magnussen RA, Gezmez F, et al. The anterolateral ligament of the human knee: an anatomic and histologic study. *Knee Surg Sports Traumatol Arthrosc*. 2012;20:147-152.